第 34 卷第 7 期
2018 年 7 月

无 机 化 学 学 报
CHINESE JOURNAL OF INORGANIC CHEMISTRY

Vol.34 No.7
1351-1364

高性能 T 型沸石膜的合成及水热/耐酸性能

罗益韦[1] 潘恩泽[1] 褚晶晶[1] 杨建华*,[1] 王金渠[2] 贺高红[2] 鲁金明[1]
([1]大连理工大学精细化工国家重点实验室,吸附与无机膜实验室,大连 116024)
([2]大连理工大学石油化工学院,精细化工国家重点实验室,盘锦 124221)

摘要:考察了晶种尺寸形貌及晶化温度对 T 型沸石膜的形成演化过程以及分离性能的影响,调查表明采用小尺寸的晶种可制备出致密的沸石膜,且膜的生长速率受晶化温度影响,低温下合成同性能的膜需更长的晶化时间。当晶种尺寸分别为 0.4 和 0.6 μm 时,423 K 晶化 4 h 可制得高性能的 T 型沸石膜,348 K 分离 90%(*w*/*w*) 异丙醇/水混合物体系,其通量分别高达 6.21 和 5.98 kg·m^{-2}·h^{-1},分离因子均>10 000。实验发现,膜的形成过程受外延生长机理控制,与晶种形貌尺寸和晶化温度无关,且所制得的高性能 T 型沸石膜具有很好的水热稳定性及耐酸性。

关键词:T 型沸石膜;渗透蒸发;取向;水热/耐酸稳定性
中图分类号:O613.72 **文献标识码**:A **文章编号**:1001-4861(2018)07-1351-14
DOI:10.11862/CJIC.2018.156

Synthesis and Hydrothermal/Acid Stability of High Performance Zeolite T Membrane

LUO Yi-Wei[1] PAN En-Ze[1] CHU Jing-Jing[1] YANG Jian-Hua*,[1]
WANG Jin-Qu[2] HE Gao-Hong[2] LU Jin-Ming[1]
([1]*State Key Laboratory of Fine Chemicals, Institute of Adsorption and Inorganic Membrane, School of Chemical Engineering, Dalian University of Technology, Dalian, Liaoning* 116024, *China*)
([2]*State Key Laboratory of Fine Chemicals, School of Petroleum and Chemical Engineering, Dalian University of Technology, Panjin, Liaoning* 124221, *China*)

Abstract: The influences of seed crystals and crystallization temperatures on the formation evolution and performance of zeolite T membranes were investigated, revealing that dense membranes could be obtained by using smaller seeds and the membrane growth rate was significantly affected by crystallization temperature. High performance zeolite T membranes with flux of 6.21 and 5.98 kg·m^{-2}·h^{-1} respectively and high separation factor (>10 000) for 90%(*w*/*w*) isopropanol solution at 348 K were obtained by using 0.4 and 0.6 μm seeds at 423 K for 4 h. A much long synthesis time was required at low temperature for achieving similar separation performance. It was found that the membrane formation was governed by the same mechanism of epitaxial growth, independent on the seed size and morphology and the crystallization temperature for the investigated synthesis solution. Furthermore, the zeolite T membranes show good hydrothermal and acid stability.

Keywords: zeolite T membrane; pervaporation; orientation; hydrothermal/acid stability

收稿日期:2018-01-30。收修改稿日期:2018-04-25。
国家自然科学基金(No.21376036,21236006)、国家高技术研究发展计划(No.2015AA03A602)和中央高校基础研究基金(No.DUT15ZD(G)03)项目资助。
*通信联系人。E-mail:yjianhua@dlut.edu.cn

0 Introduction

The conventional purification techniques such as distillation, drying and evaporation are energy-intensive operations, especially for separating azeotropic and close-boiling liquid mixtures[1-2]. With growing concern for energy consumption and cost expenditure, membrane-based separation techniques are widely used for gas and liquid mixtures due to the low energy requirement and environmental friendness[3-6]. Among the membrane separation, membrane pervaporation (PV) is emerging as viable options for separating azeotropic and close-boiling liquid mixture. Compared to polymer membranes, inorganic membranes draw increasing attentions due to their good thermal, mechanical and chemical stability [7-8], particularly zeolite membranes with various Si/Al molar ratio and molecular sieving selectivity show potential application in separation of many industrially important mixtures, which allow them to do PV under harsh conditions[9-12].

The dehydration of organic mixtures is essential in many industrial process including petrochemical, organic chemicals, pharmaceutical chemicals and biotechnology industries. Zeolite LTA (LTA type of zeolite framework) membranes have low Si/Al molar ratio of 1 and high hydrophilicity, thus, LTA type zeolite membranes[13-16] show high pervaporation performance on organic/water mixtures and have been industrially applied for the dehydration of aqueous organic solutions on a large scale. However, zeolite LTA membranes[17] are unstable under acidic conditions due to Al content in the zeolite LTA framework dissolving in an acidic media. Therefore, development of the zeolite membranes with high hydrophilicity and acid resistance are in great demands.

The controlling of membrane microstructures including preferential grain orientation[18-19], the membrane morphology[20], the membrane thickness[21], and grain boundary defects[22] is key to the formation of a high performance zeolite membrane. Recently, it is noted that among the microstructures, the orientation of zeolite membranes is found to have significant effects on the separation performance, many efforts[23-27] have been made to study the orientation of zeolite membranes. Lai et al. [25] obtain *b*-oriented, *b*&*a*-oriented, *b*&*a*&*h*0*h*/*c*-oriented ZSM-5 membranes through controlling the synthesis conditions and finally affected the membrane microstructure and separation performance, indicating that the membrane performance strongly depended on the membrane orientation. Huang et al.[24] prepare a highly oriented $AlPO_4$ LTA monolayer on porous α-Al_2O_3 supports by secondary growth, which significant improves the separation performance. It can be expected that the orientation of membrane is key to the performance of zeolite membranes.

Zeolite T[14,25,28] has a medium Si/Al molar ratio of 3 ~4 which are found to be acid resistance while remaining relatively high hydrophilicity, therefore zeolite T membranes show great potential applications in pervaporation dehydration organics in acid conditions and attract great attentions. The *a*&*b*-oriented zeolite T membranes with water flux of 2.15 $kg \cdot m^{-2} \cdot h^{-1}$ and separation factor of 10 000 for dehydration of 90% (*w*/*w*) isopropanol solution at 338 K were obtained by Yang et al.[29] They make the ~8.5 μm rod-like zeolite T seeds lay on the support surface with their *c*-axis parallel to support surface, and then synthesize the *a*&*b*-oriented zeolite T membranes by combining the conventional heating with microwave heating, which improves the membrane performance. Chen et al.[30] obtain mostly *c*-oriented zeolite T membranes from clear solutions at 423 K for 35 h, while the flux and separation factor for 90% (*w*/*w*) isopropanol solution were 2.5 $kg \cdot m^{-2} \cdot h^{-1}$ and 13 000 at 338 K respectively, which still need to improve. Then they[31] prepare high water flux around 6.7 $kg \cdot m^{-2} \cdot h^{-1}$ of zeolite T membranes on stainless steel supports by adding F^- into synthesis solutions. Gu et al.[32] synthesize high flux of 7.36 $kg \cdot m^{-2} \cdot h^{-1}$ for 90% (*w*/*w*) isopropanol solution zeolite T membranes on YSZ hollow fibers with a long crystallization time >30 h. Wang et al.[33] obtain zeolite T membranes with a flux of 12.2 $kg \cdot m^{-2} \cdot h^{-1}$ and separation factor of >10 000 for 90% (*w*/*w*) isopropanol solution at 348 K by ultrasonic assisted pretreatment. However, all these zeolite T membranes require a long synthesis time about 30 h or with F^-

ions or ultrasonic assisted in the synthesis gel that are not environmentally friendly.

Zeolites T is an intergrowth of offretite (60%~97% (*w*/*w*)) and erionite, in their structure, each erionite cage involves a large pore (12-ring) in *c*-direction completely blocked by 6-ring channels with opening channel for molecular permeation small to 0.25 nm, which results in a "dead-end" effect to the large pore of offretite[34]. This effect force the molecule diffusion through 8-ring channel in the a or *b*-direction (perpendicular to *c*-direction) with free diameter of 0.31 nm, leading to the shape-selectivity[24]. Thus, small amount of erionite intergrown in offretite is expected to key control even the offretite can absorb large molecules into zeolite. Therefore, principally the preferred orientation for the water molecular (0.28 nm) permeation is a or *b*-axis for zeolite T, the *a*&*b*-oriented zeolite T membranes are supposed to possess high separation performance.

By controlling of the crystallization behavior of zeolite T membrane, we[35] recently realize an epitaxial growth for synthesizing an *a*&*b*-oriented zeolite T membranes on the Al_2O_3 hollow fibers and macroporous alumina supports, high flux and selectivity of the as-synthesized zeolite T membrane for dehydration of isopropanol/water mixtures were obtained together with a largely shortened synthesis time of 4 h. Compared to those zeolite T membranes reported in reference, the high performance zeolite T membranes in the present work employ the same synthesis method, which only require a short synthesis time by one step synthesis and without additives. Besides, the seeds size and shape, synthesis temperature influences on the growth and performance of the zeolite T membranes on macroporous Al_2O_3 tubes were investigated systematically to reveal the formation evolution process of the zeolite T membranes. Furthermore, their pervaporation performance for isopropanol/water mixtures and hydrothermal/acid stability were evaluated.

1 Experimental

1.1 Preparation of zeolite T seeds

Zeolite T seeds with different crystal sizes were prepared from aluminosilicate gels with molar composition of (1) $18.2SiO_2$:$1Al_2O_3$:$4.2Na_2O$:$1.5K_2O$:*x*TMAOH:$212.7H_2O$ (where x=1.5 was denoted as the S1 solution, and x=1.82 was denoted as the S2 solution) and (2) $40SiO_2$:$1Al_2O_3$:$6Na_2O$:$6K_2O$:2TMAOH:$560H_2O$ (denoted as S3 solution) by controlling the synthesis parameters. In a typical synthesis, potassium hydroxide (>85% (*w*/*w*), Sinopharm Chemical Reagent Co., Ltd.), sodium hydroxide (>96% (*w*/*w*), Tianjin Kermel Chemical Reagent CO., Ltd.) and sodium aluminate (Al_2O_3: 41% (*w*/*w*), Na_2O: 24.92% (*w*/*w*), Sinopharm Chemical Reagent Co., Ltd.) were dissolved in deionized water. Tetramethylammonium hydroxide (TMAOH) solution (25% (*w*/*w*) in water, Zhejiang Ken Te Chemical Co., Ltd.) was then added into the base solution. And then, colloidal silica Ludox AS-40 (40% (*w*/*w*) in water, Aldrich) or JN-40 (40% (*w*/*w*) in water, Qingdao Haiyang Chemical Co., Ltd.) was added dropwisely with stirring. The gel was sealed into a Teflon-lined stainless steel autoclave at a specified crystallization condition (Table 1) after aging at ambient temperature for 12 h under stirring.

Table 1　Crystallization conditions of prepared zeolite T samples and the corresponding seeded support

Suspension name	Synthesis solution	Heating[c]	Synthesis temperature / K	Synthesis time / h	Size / μm	Corresponding seeding concentration (*w*/*w*)	Corresponding seeded support sample name
A	S1[a]	CH	353	48	0.4	0.5%	L1
B	S2[a]	CH	373	48	0.6	0.6%	L2
C	S1[a]	CH	383	48	1	0.8%	L3
D	S1[a]	MH	373	8	2	1%	L4
E	S2[b]	CH	373	48	3	2%	L5
F	S3[a]	CH	403	120	~0.5	0.6%	—

[a] Colloidal silica Ludox AS-40; [b] Colloidal silica JN-40; [c] CH: conventional hydrothermal synthesis; [c] MH: Microwave hydrothermal synthesis (Microwave equipment: MDS-6, Sineo Microwave Chemistry Technology (Shanghai) CO., Ltd.).

The resultant products were purified by centrifugation four times followed by ultrasonic redispersion in deionized water. The rinsed product was dried at 373 K overnight and then calcined in air at 823 K for 6 h.

1.2 Preparation of seeds layer

Macroporous Al_2O_3 tubes with 2~3 μm thickness Al_2O_3 powders on the outer surface diameter of 12 mm, thickness of 2 mm and outer length of 50 mm (Foshan Ceramics Research Institute, China) were used as supports. The outer surfaces of the tubes were polished with 800 and 1 500 mesh SiC paper. Then, the supports were sonicated for 15 min to remove the loose particles. Subsequently, the supports were washed in an ultrasonicator with acid solution, alkaline solution, and deionized water in turn. To burn off the organics on the support surface, the cleaned supports were calcined in air at 823 K for 6 h.

Zeolite T seeds were dispersed in deionized water to get required seeding suspensions. The preheated (393 K for 3 h) tubes with two ends sealed by Teflon plugs were firstly dipped into suspension D (1%, 2 μm) for 20 s, followed by drying in room temperature and then heating in an oven at 448 K for 3 h. The outer surface of the dried support was rubbed using cotton to remove superfluous and loose seeds. After that, the rubbed support was preheated in an oven again at 373 K for 2 h and then dipped into suspension B (0.6%, 0.6 μm) for 20 s, and followed by drying at 373 K for 2 h. For comparison, the second dipping suspensions can be replaced by suspension A (0.5%, 0.4 μm), C (0.8%, 1 μm), D (1%, 2 μm), E (2%, 3 μm) and F (0.6%, ~0.5 μm), respectively. Detailed seeding concentrations and the corresponding seeded support samples were denoted as shown in Table 1.

1.3 Preparation of zeolite T membranes

The seeded support tube was sealed with Teflon caps at both ends and placed vertically in a Teflon autoclave filled with an organic template-free synthesis solution. The molar composition of the synthesis solution $n_{SiO_2}:n_{Al_2O_3}:n_{Na_2O}:n_{K_2O}:n_{H_2O}$ was $1:0.05:0.26:0.09:35$ ($1SiO_2:0.05Al_2O_3:0.26Na_2O:0.09K_2O:35H_2O$) obtained by mixing aluminate solution with silica sol. The aluminate solution was prepared by dissolving potassium hydroxide and sodium hydroxide in deionized water, then adding sodium aluminate into the solution until the solution became clear. Subsequently, the silica solution was added dropwisely. The synthesis solution was aged in water bath and vigorously stirred for 24 h at 298 K. The resulted autoclave containing the seeded support and synthesis solution was moved to a 423 K preheated oven for 4 h crystallization reaction. The resultant membrane was thoroughly washed with water and dried at 373 K for several hours. For comparison experiments, the detailed synthesis conditions and their corresponding sample name were listed in Table 2.

1.4 Characterization of zeolite T membranes

The morphologies of zeolite T seeds and as-synthesized membranes were characterized by X-ray diffraction (XRD) with a D/MAX-2400. X-ray diffraction

Table 2 Synthesis condtions of prepared zeolite T membranes

Membrane name	Second time seeding solution	Synthesis temperature / K	Synthesis time / h	Membrane name	Second time seeding solution	Synthesis temperature / K	Synthesis time / h
M1	Suspension A	423	4	M11	Suspension B	373	24
M2	Suspension B	423	4	M12	Suspension B	373	25
M3	Suspension C	423	4	M13	Suspension B	373	30
M4	Suspension D	423	4	M14	Suspension B	393	3
M5	Suspension E	423	4	M15	Suspension B	393	6
M6	Suspension F	423	4	M16	Suspension B	393	9
M7	Suspension B	373	4	M17	Suspension B	393	12.5
M8	Suspension B	373	10	M18	Suspension B	393	13
M9	Suspension B	373	16	M19	Suspension B	393	13.5
M10	Suspension B	373	23	M20	Suspension B	393	15

meter using Cu $K\alpha$ radiation (λ=0.154 nm, 30 mA and 40 kV, scan range 2θ=5°~45°) and scanning electron microscopy (SEM) using a QUANTA 450 at an acceleration voltage of 20 kV.

1.5 Pervaporation measurements of the prepared zeolite T membranes

The prepared zeolite T membranes were tested by PV apparatus which was illustrated in our previous report[36]. The pervaporation (PV) measurements for isopropanol/water ($w_{isopropanol}/w_{water}$=9, the same below) were performed at 348 K (acid stability is tetrahydrofuran/water ($w_{tetrahydrofuran}/w_{water}$=96.7/3.5, added HCl, pH<1 at 333 K) mixture evaluated at 333 K for 219 h). The feed side was stirred vigorously and the permeate side was kept under vacuum of 70~80 Pa. The permeating vapor was collected by a cold trap cooled by liquid nitrogen. The feed and permeate composition were measured by a gas chromatograph (GC) using a GC7890T. The PV performance of membranes were evaluated by permeation flux Q, kg·m^{-2}·h^{-1} and separation factor (S.F.) α. The permeation flux was calculated by the mass of permeate in each time interval. The S.F. is defined as

$$\alpha_{w/o}=(y_w/y_o)/(x_w/x_o)$$

where x_w, x_o, y_w and y_o denote the mass fractions of water (w) and organic (o) in the feed and permeate sides, respectively.

2 Results and discussion

2.1 Prepared zeolite T seeds

Crystallization conditions were found to significantly affect the zeolite crystal morphology, such as changing the crystallization temperature, increasing the ratio of the template, changing the way of heating etc. Zeolite T crystals were reported to be synthesized in different conditions[37-38], here, zeolite T seeds with different crystal size 0.4 ~3 μm and shape were obtained by varying synthesis conditions as listed in Table 1. SEM images are shown in Fig.1. It is observed that seeds A, B, C, D and E are all uniformly rice-shaped. Seeds F has a spherical shape with uniform size. These particle suspensions were used to prepare the seeding layer. The XRD patterns of the prepared zeolite T seeds A, B, C, D and E are shown in Fig.2. All the peaks of seeds observed in the XRD patterns can be associated with zeolite T and no other peak appeares, illustrating that all the seeds are pure T-type zeolite phase. Besides, the prepared seeds are of highly crystalline pure zeolite T considering that the complete seeds morphology from Fig.1. It is noted that the intensity of seeds F are much higher than other seeds, which probably because of the spherical shape of seeds F providing more structure information for XRD tests.

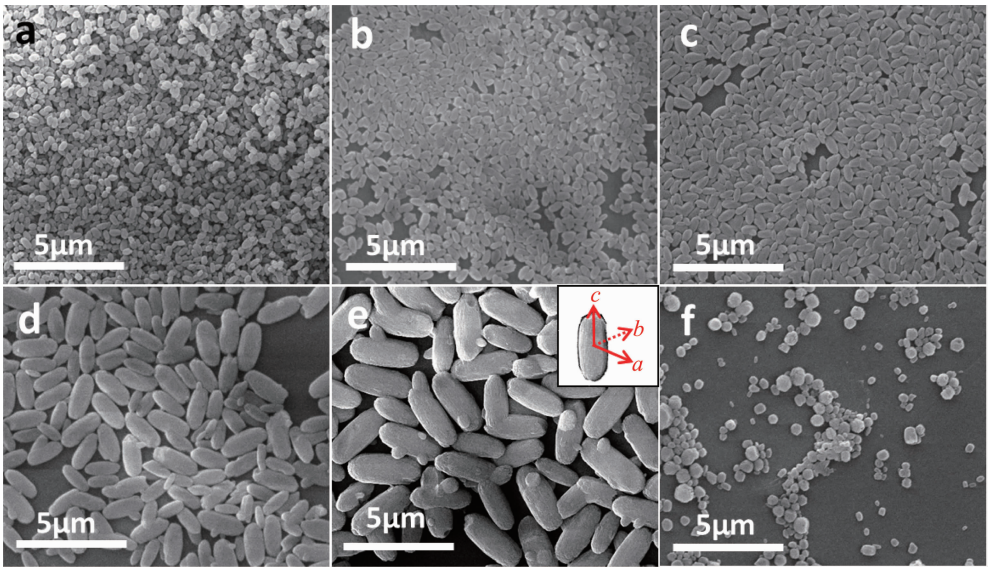

Fig.1 SEM images of zeolite T seeds of (a) A, (b) B, (c) C, (d) D, (e) E and (f) F

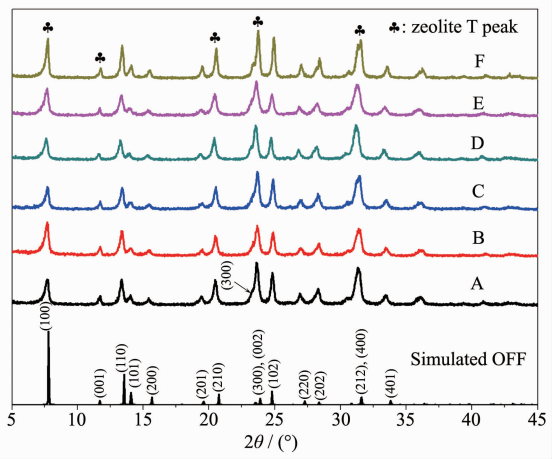

Fig.2 XRD patterns of simulated zeolite offretite (OFF) and zeolite T seeds

2.2 Effects of seeds size on zeolite T membrane formation

It is well known that the seeds particle size strongly influences the morphology and the formation of zeolite membrane. Engstrm and co-workers[39] synthesize preferred silicalite-1 films on gold surface by using different sizes of zeolite seeds. They propose that the seeds consisted of mother crystals with 90° rotational intergrown daughter crystals and no additional crystals attached to the film during growth, resulting in the predominantly oriented films with a-axis perpendicular to the surface despite the different sizes of the seeds (60, 165 and 320 nm). However, the SEM images of the film surface show different morphologies. Here, 3, 2, 1, 0.6 and 0.4 μm zeolite T crystals with corresponding seeds concentration (Table 1) were used as the seeds to investigate the effects of seeds size on the formation of zeolite T membranes.

Fig.3 shows the SEM images of top view and cross section of as-synthesized zeolite T membrane at 423 K for 4 h and their corresponding cross section of seeds layer with different seeds size. It is interesting that the zeolite T membrane morphologies prepared by different seeds sizes are quite distinct. When the seeds size is 3 μm, wheat-like shape crystals fully cover on the support surface for the membrane M5 (Fig.3i). As zeolite T seeds size decreasing, crystal sizes on the membrane surface also decrease with their morphology changing from wheat-like (Fig.3(g,i)), stick-like (Fig.3e) to rod-like (Fig.3(a,c)). At the same time, the crystals on all the synthesized membrane layer lay on the surface with their long direction parallel to the support surface, and their radius perpendicular to the long direction close to their corresponding seeds size respectively, except the length of the crystals along the long direction is longer than that of the seeds. This reasonably results from the *c*-axis preferred orientation growth (*c*-axis is denoted along the long direction of crystals, *a*- and *b*-axis are denoted identical perpendicular to the long direction, as shown in Fig.1e). Moreover, the larger sizes of zeolite T crystals, such as M5 (3 μm), and M4 (2 μm), inducing more intercrystalline grain boundary defects cross the membrane. Gaps between intergrown crystals can be obviously observed in Fig.3 (g ~j). Those defects would cause poor separation performance for the pervaporation dehydration. As shown in Fig.3, with a decrease of the seeds size, less grain boundary defects are generated on the membrane layer. For the synthesized membranes with 0.6 and 0.4 μm zeolite T seeds, well intergrown zeolite layers are formed on the supports (Fig.3(a~d)). It is speculated that the smaller zeolite T seeds are more suitable for growing denser zeolite T membranes large seeds. This can be ascribed to the high density of small seeds covering on the support surface, and thus less voids would exposure between seeds crystals, finally benefiting to seeds growing and closing voids, forming a dense, non-defects and uniform membrane (the detail membrane growth process will discuss in the late sessions).

Fig.4a shows XRD patterns of all the synthesized membranes, which all displayed similarly strong Al_2O_3 support peaks but low zeolite T peaks with stars (*) (peaks at 2θ=7.7°, 13.3°, 20.4°, 23.7°and 31.4°). The weak peaks are probably due to the thin membrane layer. The intensitiy of zeolite T peaks in membrane M4 and M5 is higher than that of M1, M2 and M3, which might be ascribed to the thickness of those two membranes larger than that of others as observed from cross sections of SEM in Fig.3. Besides, no other peaks are detected in the XRD patterns, indicating

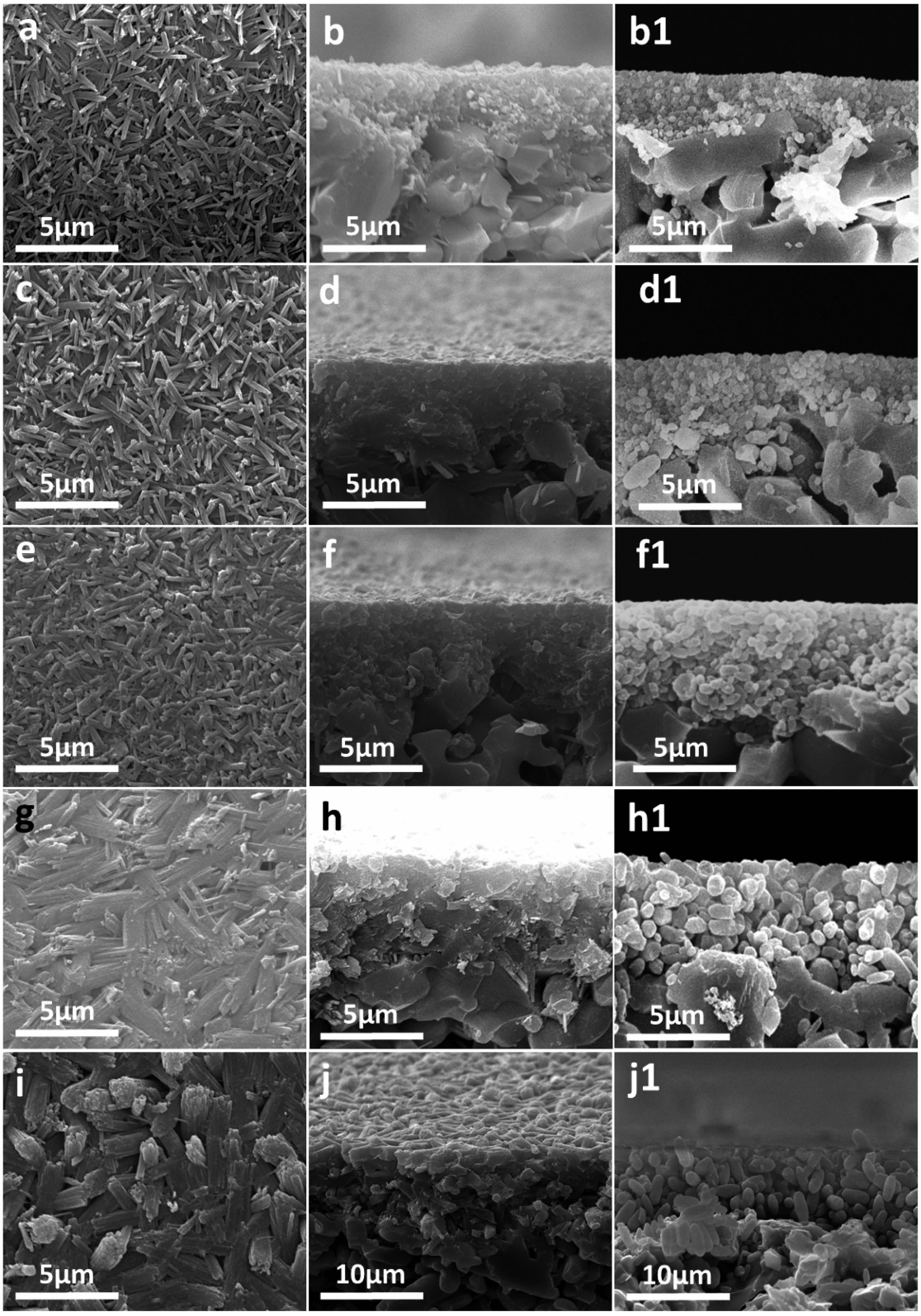

(a, b) for M1 and (b1) for L1, (c, d) for M2 and (d1) for L2, (e, f) for M3 and (f1) for L3, (g, h) for M4 and (h1) for L4, (I, j) for M5 and (j1) for L5

Fig.3　From left to right, SEM images of top view and cross section of prepared zeolite T membranes and their corresponding cross section of seeds layer with different seeds sizes

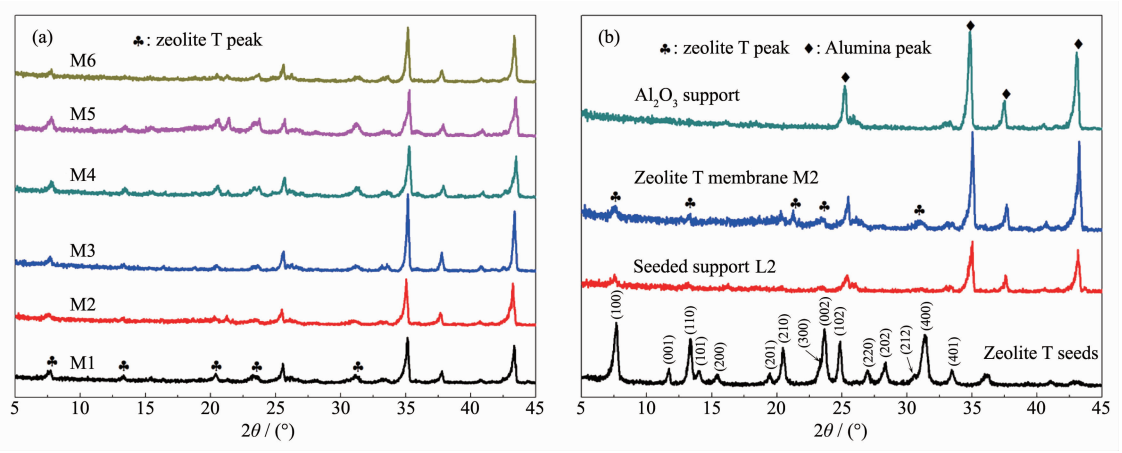

Fig.4 XRD patterns of (a) the prepared zeolite T membranes with different seeds size and (b) Al_2O_3 support, the prepared zeolite T membrane M2, the seeded support L2, and the zeolite T seeds B

that no other impure phase zeolite formed during the membrane growth. Taking into consideration of the synthesis conditions and the similar peak intensities in XRD pattern, it can be concluded that all the as-prepared membranes were *a*&*b* orientation despite of the size of the seeds from 0.4 to 3 μm. In order to clearly observe the orientation, XRD patterns of zeolite T membrane M2 with its corresponding seeds B, seeded support L2 and support are drawn in Fig.4b. Compared to the seeds, the peak of (001) plane for the membrane and the seeded support is missing, all peaks of (201), (102) and (202) planes become weak, and the peak intensity of $I_{(300)}$ to $I_{(002)}$ increased, indicating that both the seeds layer and the membrane are mostly oriented with their *a*- and *b*-plane perpendicular to the support surface. Therefore, the oriented seeds layer finally induced the oriented membrane layer. Moreover, the membrane thickness remain almost the same with the seeds layer (Fig.3), which also demonstrates that the epitaxial membrane growth[35].

The effects of seeds size on PV performance of 90% isopropanol solution at 348 K through the synthesized membranes are displayed in Table 3. The flux of membrane M1 and M2 were 6.21 and 5.98 kg·m^{-2}·h^{-1} with corresponding separation factors greater than 10 000, displayed better PV performance than the membrane M3, M4, and M5. Apparently, the smaller seeds membrane (size 0.4~0.6 μm) show good separation PV performance, verifying smaller seeds leading to a dense zeolite membrane layer formed on the support. Poor separation performance of membranes are obtained with increasing seeds size (1~3 μm), which is probably due to the grain boundary gaps that

Table 3 Effects of seeding size on PV performance of prepared zeolite T membranes

Membrane	Q / (kg·m^{-2}·h^{-1})	Separation factor	Membrane	Q / (kg·m^{-2}·h^{-1})	Separation factor
M1	6.21	>10 000	M11	6.36	895
M2	5.98	>10 000	M12	6.53	272
M3	5.53	595	M13	5.44	317
M4	7.66	29	M14	—	—
M5	9.09	16	M15	14.51	14
M6	5.65	501	M16	12.67	20
M7	—	—	M17	5.77	>10 000
M8	13.22	6	M18	6.74	910
M9	8.10	93	M19	7.16	120
M10	5.64	>10 000	M20	6.11	180

Pervaporation conditions: 90% (*w*/*w*) isopropanol solution at 348 K; —: no separation performance.

is in accordance with the SEM images shown in Fig.3.

2.3 Effects of seed morphology on zeolite T membrane formation

As discussed above, zeolite T membranes with good PV performance can be prepared by using smaller seeds (0.4~0.6 μm). However, all those seeds have a rice-like morphology, it was curious to know whether the particle shape will show important effects on the growth of zeolite T membrane. Thus, the ~0.5 μm spherical zeolite T crystals (Fig.1f) were used as the seeds to prepare zeolite T membrane M6. SEM images in Fig.5 reveals that the as-synthesized membrane M6 was fully covered with stick-like zeolite T crystals, which is similar to the surface morphology of membrane M2. The XRD pattern of the membrane M6 in Fig.4 confirms that it is an *a*&*b* orientation membrane. Moreover, the membrane (Table 3) show a separation factor of 501 with a permeation flux of 5.65 $kg \cdot m^{-2} \cdot h^{-1}$, a low dehydration performance for the dehydration of 90% isopropanol solution at 348 K, which is probably due to the random orientation for spherical-shape seeds, thus results in the poor grain intergrowth. Therefore, a&b orientation zeolite T membrane can be obtained by *c*-axis preferred growth in this work in spite of the different seed morphology.

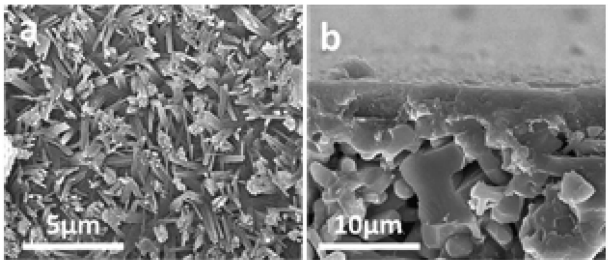

Fig.5 SEM images of top view (a) and cross section (b) of prepared zeolite T membrane for M6

2.4 Effects of crystallization temperature on membrane formation

The formation of zeolite membranes are largely affected by the synthesis temperature due to its influence on nucleation and growth rate. To further reveal the effects of crystallization temperature on the membrane growth, the zeolite T membrane growth process at different synthesis temperature were investigated. Fig. 6 and 7 (M7~M17) show the morphologies of the zeolite T membranes prepared at 373 and 393 K respectively for different synthesis time. At 373 K, some small particles emerged on the seed crystals

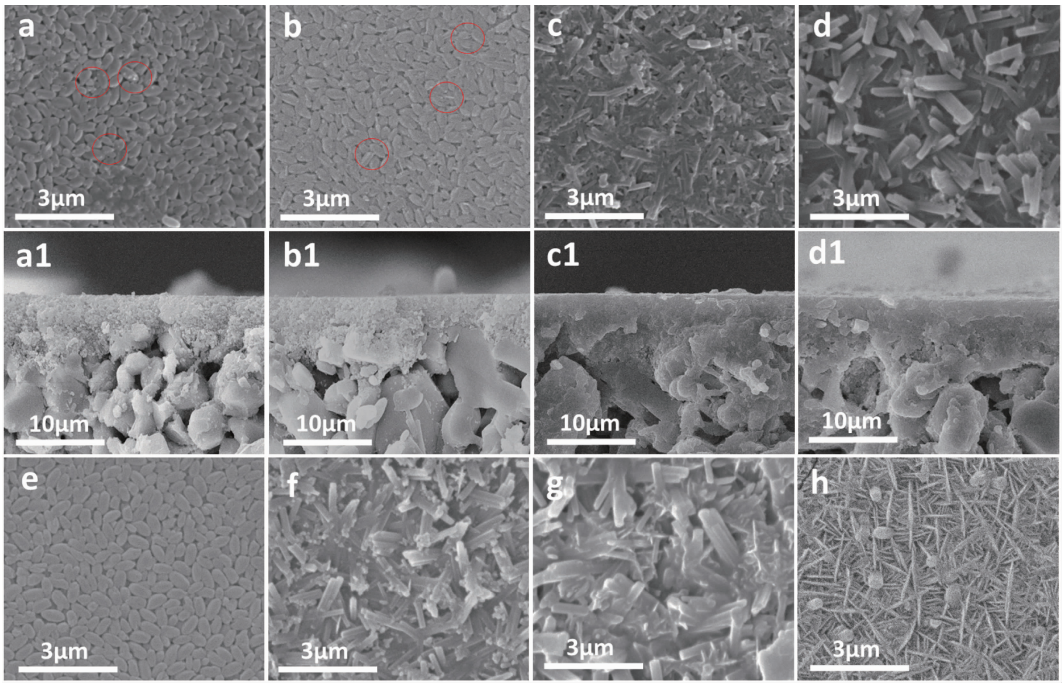

(a, a1) for M7, (b, b1) for M8, (c, c1) for M9, (d, d1) for M10, (e) for L2, (f) for M11, (g) for M12, and (h) for M13

Fig.6 SEM images of top view (top and bottom) and cross section (middle) of prepared zeolite T membranes at 373 K for different synthesis time

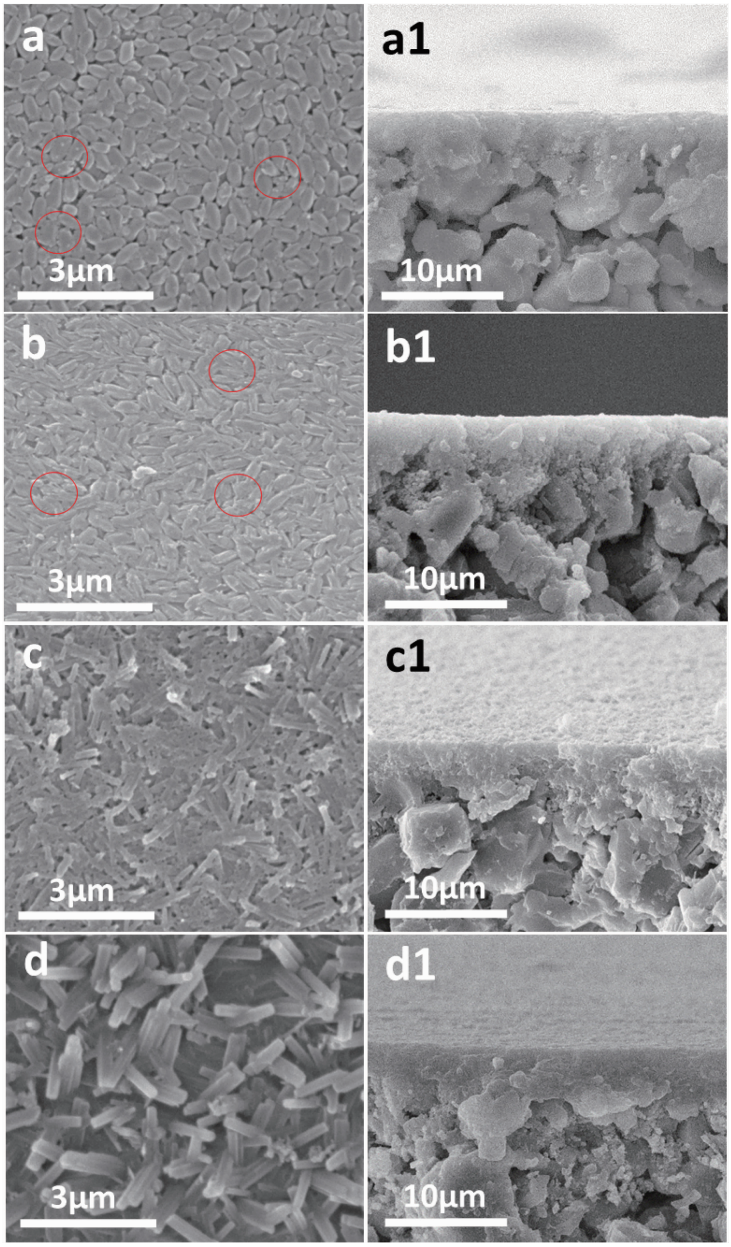

(a, a1) for M14, (b, b1) for M15, (c, c1) for M16, and (d, d1) for M17

Fig.7 SEM images of top view (left) and cross section (right) of prepared zeolite T membranes at 393 K for different synthesis time

(Fig.6a as marked by red circle) after 4 h crystallization compared to the seeds layer Fig.6e, the similar phenomenon is observed in Fig.7(a,a1) at 393 K for 3 h. With increasing in synthesis time to 10 h at 373 K and 6 h at 393 K, the seeds on both two membranes become larger and interconnected and the voids become smaller. The significant changes are observed during those time, the seeds become well intergrown with a rod-like "tail" elongating to some rice-like seeds (as marked by the circles in Fig.6), while the membrane thickness during the process remained almost the same 3~5 μm (Fig.3d1). It is interesting that the rod-like "tail" appeared more obviously at 393 K even for a shorter time 6 h than 373 K for 10 h during the membrane grow process, which might be because of the high crystal growth rate under high synthesis temperature. At 373 K for 16 h, the membrane surface was compactly covered by highly intergrown rod-like crystals, similar to the surface at 393 K for 9 h. When extending the time to 23 h at

373 K and 12 h at 393 K, dense and uniform membrane layer were obtained with seeds completely intergrown. After that, even just increased 2 h at 373 K and 1 h at 393 K, the regular-shaped zeolite T crystal phases on the membrane easily transformed to another type of crystal phase (XRD demonstration show in Fig.8). The morphology of membrane 393 K for 13, 13.5 and 15 h were similar to the 373 K for 24, 25 and 30 h respectively, so, the SEM images of 393 K for 13, 13.5 and 15 h are not shown here. After 24 h in Fig.6, the rod-like and new sheet-round shape crystals intergrown on the membrane surface. Surprisingly many small particles appeared on the membrane surface before the crystal shape changed at 24 h, which might have appeared to form the new type of crystals. The transformation phenomenon could be due to the metastable state of zeolite T crystals in the hydrothermal synthesis environment. Similarly, Chen et al.[40] report that chabazite membranes are prepared by secondary growth using zeolite-T-directed chabazite seeds in hydrothermal systems.

The XRD patterns of the prepared membranes M7~M13 at 373 K for 4~30 h show that the intensity of the peaks of (100), (110), (210) and (220) planes are strengthened as prolonging the crystallization time, indicating that the coverage and density of *a*&*b*-orientated zeolite T membranes increased. The peak of (001) plane is lost and the peaks of (201), (102) and (202) planes become very weak and almost missing. In addition, the peak intensity of $I_{(300)}$ to $I_{(002)}$ for the prepared membrane at 373 K for 23 h increased compared to seeds B. All these facts confirm the epitaxial membrane growth in our work. It is interesting that Yang et al.[29] also synthesize *a*&*b*-oriented zeolite T membranes by microwave-assisted hydrothermal synthesis method, revealing different membrane growth process, namely, new zeolite T crystals formed among the originally coated seeds resulting in their quickly growth and sealing the gaps of the seed layer, finally formed the orientation membrane. Here, however, with the crystallization time increased from 24 to 30 h, the intensity of zeolite T peaks decrease, *i.e.* Zeolite T phase decreased, that is corresponding to the SEM images (Fig.8). Moreover, the alumina peaks decreased after 24 h, likely due to the new formed phase (amorphous medium phase) covers the surface, leading to weaker XRD intensity. Besides, other peaks were detected at the 5.34° and 8.56° as marked arrow in Fig.8, demonstrating that impure zeolite phase is formed. The XRD patterns for the membranes prepared at 393 K are not shown here since they show the similar results. It is worth noting that the XRD of the sample (not shown here) collected from the bottom of autoclave for the membrane M10 and M17 exhibit amorphous phase structure, indicating that no T crystals form by the homogeneous growth in the solution, which provids proof for the heterogeneous growth of seeds for the resulting zeolite T membrane.

The PV flux and the separation selectivity for separation of 90% isopropanol solution at 348 K are given in Table 3, displaying that the obtained

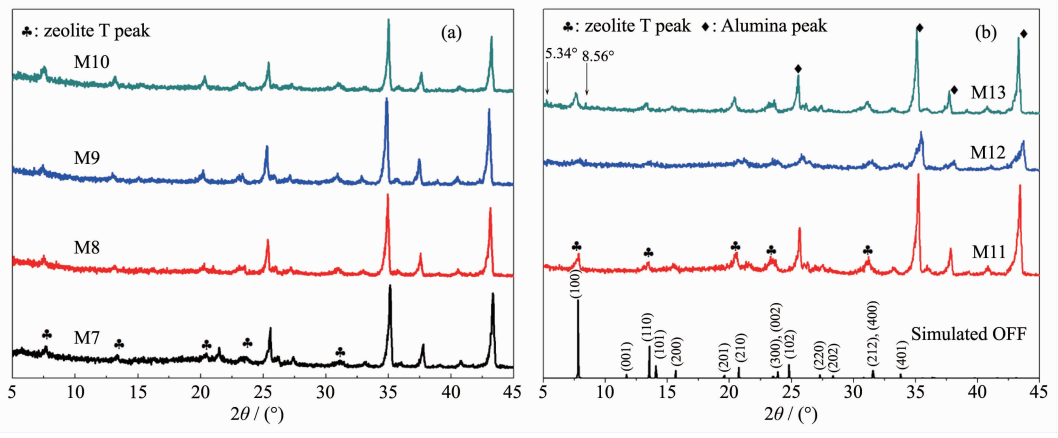

Fig.8　XRD patterns (a, b) of the prepared zeolite T membranes at 373 K for different times and simulated zeolite OFF

separation performance is consistent with the SEM and XRD results as mentioned above. When the synthesis time were as short as 4 h at 373 K and 3 h at 393 K, the membranes were non-selective. The selectivity increases with the extending of the synthesis time, attributing to the zeolite T crystals growing and the gaps decreasing. At the crystallization time up to 23 h at 373 K and 12.5 h at 393 K, the membranes show good separation performance with separation factor more than 10 000 and high flux of 5.64 and 5.77 kg·m^{-2}·h^{-1}, respectively. Then the separation performance decreases due to the presence of new phases generated on the surface of the membranes.

According to the above tracking observations of SEM and XRD, together with the membrane PV performance, the membrane growth process for the different crystallization temperatures are almost the same, even similar to that of high temperature at 423 K[35]. At the early stage <10 h at 373 K, <6 h at 393 K and <2 h at 423 K, the seeds grow along *a*&*b*-direction, resulting in the size increase of the seed grains and the closing of seed voids. During this time, few new nuclei appeared on the seeds layer, which could be the nucleation process. However, judging by the unchanged membrane thickness, the newly formed nuclei are dissolved into the solution to provide nutrient for the crystal growth according to Ostwald ripening[41]. At certain critical time when the "tail" appeared, the seeds preferentially grew in the *c*-direction, leading to the formation of rod-like crystals. The critical time was dependent on the crystallization temperature, a longer time required at the lower temperature due to the lower crystal growth rate at lower temperature. On the contrary, a longer time was required to achieve a final dense membrane, 373 K for 23 h, 393 K for 12.5 h while 423 K for 4 h. The membrane formation process at different synthesis temperature reveal the same growth mechanism for the as-synthesized zeolite T membranes with the hydrothermal conditions for the used synthesis solution, namely, the seeds are governed by an epitaxial growth of seeds with closing of the voids between the seeds despite the different synthesis temperature during 373~423 K[35]. It is really interesting to understand what factors bring the crystal growth direction of the zeolite T changing from a&b-direction to c-direction. Further studies are required to clarify transformation reason of the preferential direction. Such microstructure manipulation for zeolite membranes will not only benefit to achieve high performance but also largely improve the productivity, these two aspects are both significant for practical industrialization application. In summary, high performance zeolite membranes can be obtained via the epitaxial growth of the zeolite T membrane, but the synthesis time is largely affected by the temperature, only 4 h at 423 K, 12.5 h at 393 K and 30 h at 373 K.

2.5 Hydrothermal stability

It has been reported that zeolite A membranes are unstable for long time PV tests due to the damages from water[42]. It is interesting to know if zeolite T membranes will be stable in the water dehydration tests for a long time. The time-dependency of 90% isopropanol solution at 348 K for 179 h shown in Fig. 9 displays that the total flux (Q) decreases from the initial value of 5.98 kg·m^{-2}·h^{-1} to a steady-state of 3.4 kg·m^{-2}·h^{-1}, and the water permeate concentration remained at 100% (*w*/*w*) through the whole test experiment. Therefore, the as-synthesized zeolite T

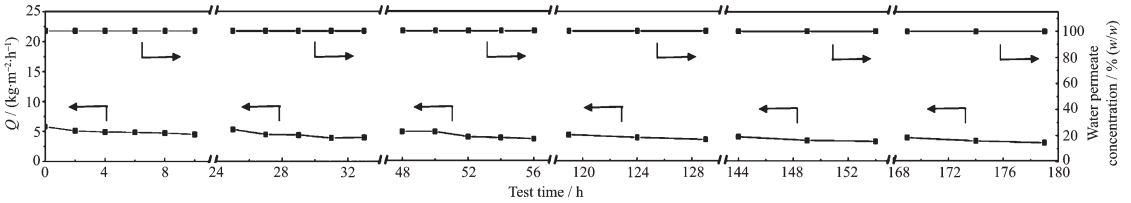

Horizontal axis break means during those time the membrane is still immersed in the solution at certain test temperature (only without vacuum pumping with other condition exactly the same with the PV measurement)

Fig.9 PV performance of zeolite T membrane as a function of operation time for a 90% isopropanol solution at 348 K

membranes are quite stable and exhibit high separation performance during the PV experiment. Compared with the zeolite A membranes reported by researchers[17], the as-synthesized zeolite T membranes exhibit high hydrothermal stability, which could be ascribe to their Si/Al ratio and higher synthesis temperature.

2.6 Acid stability for tetrahydrofuran/water acid mixtures

Considering the widely application of the zeolite T membranes for acidic environment, the water dehydration stability from a tetrahydrofuran/water ($w_{tetrahydrofuran}/w_{water}$=96.7/3.5, added HCl, pH<1 at 333 K) mixture was evaluated at 333 K for 219 h (Fig.10). The total flux through the zeolite T membranes stabilized at about 0.7 kg·m^{-2}·h^{-1}, and the water permeate concentration remained above 99.3% (*w*/*w*) through the whole test experiment. Therefore, the as-synthesized zeolite T membranes are stable. Acetic acid is not detected in permeate, neither. As concluded above, the synthesized zeolite T membranes are hydrothermal stability for both isopropanol/water ($w_{sopropanol}/w_{water}$ =9) mixtures and tetrahydrofuran/water ($w_{tetrahydrofuran}/w_{water}$=96.7/3.5, pH<1) mixtures.

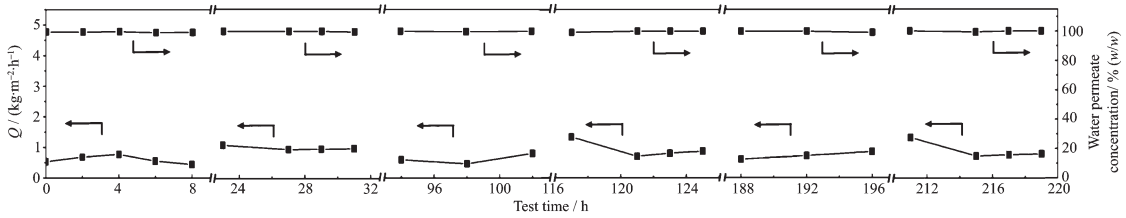

Horizontal axis break means during those time the membrane was still immersed in the solution at certain test temperature (only without vacuum pumping with other condition exactly the same with the PV measurement)

Fig.10　PV performance of zeolite T membrane as a function of operation time for a tetrahydrofuran/water ($w_{tetrahydrofuran}/w_{water}$=96.7/3.5, added HCl, pH<1 at 333 K) mixture at 333 K

3 Conclusions

In the present work, dense membranes can be obtained by using smaller seeds 0.4 to 0.6 μm and the membrane performance is significantly affected by seeds size varying from 0.4 to 3 μm. High performance zeolite T membranes with flux of 6.21 and 5.98 kg·m^{-2}·h^{-1} respectively and separation factor of >10 000 for 90% isopropanol solution at 348 K were obtained by using 0.4 and 0.6 μm seeds at 423 K for 4 h. A longer synthesis time is required at low temperature for achieving similar separation performance due to the different growth rate at different crystallization temperatures. The formation process of zeolite T membranes at 373 and 393 K reveal the same membrane growth mechanism, namely via epitaxial growth of seeds and the closing of the voids between the seeds. This growth mechanism are not affected by the crystallization temperature by using the same hydrothermal conditions as n_{SiO_2}:$n_{Al_2O_3}$:n_{Na_2O}:n_{K_2O}:n_{H_2O}=1:0.05:0.26:0.09:35 and 0.6 μm rice-like seeds, leading to dense membranes formation when exposing less voids between smaller seeds crystals. The zeolite T membranes prepared at 373 K for 23 h and 393 K for 12.5 h displayed high flux of 5.64 and 5.77 kg·m^{-2}·h^{-1} respectively and high separation factor both of them (>10 000) for 90% isopropanol solution at 348 K. Their good hydrothermal and acid stability have great potential for zeolite T membrane industrial applications.

References:

[1] Lipnizki F, Field R W, Ten P K. *J. Membr. Sci.*, **1999**,**153** (2):183-210

[2] Feng X S, Huang R Y M. *Ind. Eng. Chem. Res.*, **1997**,**36**(4): 1048-1066

[3] Wang H B, Lin Y S. *AlChE J.*, **2012**,**58**:153-162

[4] Chen Y, Liao Q, Li Z, et al. *AlChE J.*, **2015**,**61**(6):1997-2007

[5] Kanezashi M, OBrien-Abraham J, Lin Y S, et al. *AlChE J.*, **2008**,**54**(6):1478-1486

[6] Strathmann H. *AlChE J.*, **2001**,**47**(5):1077-1087

[7] Caro J, Noack M, Klsch P, et al. *Microporous Mesoporous Mater.*, **2000**,**38**(1):3-24

[8] KANG Shi-Zhao(康诗钊), MU Jin(穆劲). *Chinese J. Inorg. Chem.*(无机化学学报), **2006**,**22**(6):971-977

[9] Coronas J, Santamaria J. *Chem. Eng. Sci.*, **2004**,**59**(22/23): 4879-4885

[10]ZHOU Rong-Fei(周荣飞), LI Jun(李军), ZHU Mei-Hua(朱美华), et al. *Chinese J. Inorg. Chem.*(无机化学学报), **2010**, **26**(3):469-475

[11]ZHOU Rong-Fei(周荣飞), KONG You-Xin(孔佑鑫), ZHU Mei-Hua(朱美华), et al. *Chinese J. Inorg. Chem.*(无机化学学报), **2012**,**28**(5):942-948

[12]LIU Xiu-Feng(刘秀凤), LIU Wei(柳伟), ZHENG Meng-Yao(郑梦瑶), et al. *Chinese J. Inorg. Chem.*(无机化学学报), **2014**,**30**(12):2706-2712

[13]Urtiaga A, Gorri E D, Casado C, et al. *Sep. Purif. Technol.*, **2003**,**32**(1/2/3):207-213

[14]Li H Z, Wang J Q, Xu J, et al. *J. Membr. Sci.*, **2013**,**444**: 513-522

[15]Morigami Y, Kondo M, Abe J, et al. *Sep. Purif. Technol.*, **2001**,**25**(1/2/3):251-260

[16]Ye P, Zhang Y T, Wu H F, et al. *AlChE J.*, **2016**,**62**(7): 2468-2478

[17]Hasegawa Y, Nagase T, Kiyozumi Y, et al. *J. Membr. Sci.*, **2010**,**349**(1/2):189-194

[18]Lai Z P, Tsapatsis M, Micolich J P, et al. *Adv. Funct. Mater.*, **2004**,**14**(41):716-729

[19]Hedlund J. *J. Porous Mater.*, **2000**,**7**(4):455-464

[20]Lee P S, Zhang X, Stoeger J A, et al. *J. Am. Chem. Soc.*, **2011**,**133**(3):493-502

[21]Hedlund J, Jareman F, Bons A J, et al. *J. Membr. Sci.*, **2003**, **222**(1/2):163-179

[22]Choi J, Jeong H K, Snyder M A, et al. *Science*, **2009**,**40**(41): 590-593

[23]Lovallo M C, Gouzinis A, Tsapatsis M. *AlChE J.*, **1998**,**44** (8):1903-1913

[24]Huang A S, Caro J. *Chem. Commun.*, **2011**,**47**(14):4201-4203

[25]Lai Z P, Tsapatsis M, Nicolich J. *Adv. Funct. Mater.*, **2004**, **14**(7):716-729

[26]Elyassi B, Jeon M Y, Tsapatsis M, et al. *AlChE J.*, **2016**,**62** (2):556-563

[27]Aoki K, Kusakabe K, Morooka S. *AlChE J.*, **2000**,**46**(1):221-224

[28]Cui Y, Kita H, Okamoto K I. *J. Membr. Sci.*, **2004**,**236**(1/2): 17-27

[29]Zhou H, Li Y S, Zhu G Q, et al. *Sep. Purif. Technol.*, **2009**, **65**(2):164-172

[30]Zhou R F, Hu L L, Zhang Y J, et al. *Microporous Mesoporous Mater.*, **2013**,**174**:81-89

[31]Zhou R F, Zhang F, Hu N, et al. *Chem. Lett.*, **2011**,**40**:1383-1385

[32]Wang X R, Chen Y Y, Zhang C, et al. *J. Membr. Sci.*, **2014**, **455**:294-304

[33]Wang R, Ma N K, Yan Y S, et al. *J. Membr. Sci.*, **2018**,**548**: 676-684

[34]Gorring R L. *J. Catal.*, **1973**,**31**(1):13-26

[35]Luo Y W, Lv Y J, Kumar P, et al. *J. Mater. Chem.*, **2017**,**5** (34):17828-17832

[36]Chen Z, Yang J H, Yin D H, et al. *J. Membr. Sci.*, **2010**, **349**(1/2):175-182

[37]Rad M D, Fatemi S, Mirfendereski S M. *Chem. Eng. Res. Des.*, **2012**,**90**(10):1687-1695

[38]Matin K T, Bastani D, Kazemian H. *Chem. Eng. Technol.*, **2009**,**32**(7):1042-1048

[39]Engstrm V, Mihailova B, Hedlund J, et al. *Microporous Mesoporous Mater.*, **2000**,**38**(1):51-60

[40]Zhou R F, Li Y Q, Liu B, et al. *Microporous. Mesoporous. Mater.*, **2013**,**179**:128-135

[41]Johnson N J J, Korinek A, Dong C H, et al. *J. Am. Chem. Soc.*, **2012**,**134**(27):111068-111071

[42]Li Y S, Zhou H, Zhu G Q, et al. *J. Membr. Sci.*, **2007**,**297** (1/2):10-15